CONF-960813--1

SAND96-1654C

THE GROWTH OF MID-INFRARED LASERS AND $AlAs_xSb_{1-x}$ BY MOCVD

R. M. Biefeld, A. A. Allerman, and S. R. Kurtz
Department 1113
Sandia National Laboratory
Albuquerque, NM 87185-0601

Phone 505-844-1556
Fax 505-844-3211
e-mail rmbiefe@sandia.gov

THE GROWTH OF MID-INFRARED LASERS AND $AlAs_xSb_{1-x}$ BY MOCVD

R. M. Biefeld, A. A. Allerman, and S. R. Kurtz
Sandia National Laboratory, Albuquerque, NM 87185-0601

Abstract

We have grown AlSb and $AlAs_xSb_{1-x}$ epitaxial layers by metal-organic chemical vapor deposition (MOCVD) using trimethylamine or ethyldimethylamine alane, triethylantimony and arsine. These layers were successfully doped p- or n-type using diethylzinc or tetraethyltin, respectively. We examined the growth of $AlAs_xSb_{1-x}$ using temperatures of 500 to 600 ° C, pressures of 65 to 630 torr, V/III ratios of 1-17, and growth rates of 0.3 to 2.7 μm/hour in a horizontal quartz reactor. We have also fabricated gain-guided, injection lasers using AlAsxSb1-x for optical confinement and a strained InAsSb/InAs multi-quantum well active region using MOCVD. In pulsed mode, the laser operated up to 210 K with an emission wavelength of 3.8-3.9 μm.

1. Introduction

AlSb and $AlAs_xSb_{1-x}$ are of interest for their potential application as optical and electronic confinement layers in a variety of optoelectronic devices such as infrared detectors, resonant tunneling diodes, and laser diodes[1-4]. We are exploring the synthesis of these materials by metal-organic chemical vapor deposition (MOCVD) for their use in 2-6 μm, mid-infrared optoelectronic heterojunction devices. Emitters in this wavelength range have potential uses as chemical monitors and in infrared countermeasures [1-4].

Although devices using $AlAs_xSb_{1-x}$ have been successfully prepared by molecular beam expitaxy [2,3], there have been no reports to date of their successful use in devices when prepared by MOCVD. We are aware of two previous reports of the successful growth of $AlAs_xSb_{1-x}$ by MOCVD [4,5]. In one of those reports [5], no mention was made of the electrical quality or the impurity level of the materials. Although there have been several reports by others of the growth of AlSb and AlGaSb by MOCVD [5-11], only references [10] and [11] comment on impurity levels. It is well known that Al containing materials prepared using MOCVD tend to have larger concentrations of both O and C impurities when compared to the Ga containing analogues [4,10-14]. The presence of these impurities in Al containing semiconductors is due to the strength of the bond between Al and O or C when compared to the bond strength of Al to P, As, or Sb [12-14]. In our previous work we applied an analogous approach to that used for improving the carbon concentration in AlGaAs where trimethylamine alane (TMAA) and triethylgallium (TEGa) were used to prepare high purity AlGaAs by using TMAA or ethyldimethylamine alane (EDMAA) and triethylantimony (TESb) to prepare AlAsxSb1-x by MOCVD [4]. In this paper we will describe in more detail the preparation of epitaxial layers of n- and p-type and $AlAs_xSb_{1-x}$ on GaAs and InAs substrates as well as the growth of InAsSb/InAs multiple quantum well active region lasers using $AlAs_xSb_{1-x}$ optical confinement layers.

2. Experimental

This work was carried out in a previously described MOCVD system [14]. TMAA, or EDMAA, TESb and 100% arsine were the sources for Al, Sb and As respectively. TEGa, arsine and TESb were used to grow a 1000Å to 2500Å GaAsSb cap on all samples to keep the $AlAs_xSb_{1-x}$ layer from oxidizing. Hydrogen was used as the carrier gas at a total flow of 8 slpm. P-type doping was accomplished using 200 sccm to 500 sccm of diethylzinc (DEZn) diluted to 400 ppm in hydrogen. N-type doping was accomplished using tetraethyltin (TESn) held at 18 °C to 20 °C. The hydrogen flow through the TESn source was typically 20 sccm which was diluted with 350 sccm of hydrogen. Five to 20 sccm of this mixture was introduced into the growth chamber. Semi-insulating epi-ready GaAs and n-type InAs substrates were used for each growth.

AlSb samples 1-2 µm thick were grown at 500 to 600°C at either 76 torr or 200 torr with V/III ratios between 1.1 to 16. The best morphology was achieved at V/III = 15 and was independent of reactor pressure. The surface morphology of each layer was characterized by optical microscopy using Normarski interference contrast. Under this growth condition, the growth rate was 0.4 - 3.0 µm/hr for a group III transport rate of 1 to 7 x10^{-5} moles of TMAA per minute.

$AlAs_{0.16}Sb_{0.84}$ layers 0.5 - 1 µm thick and lattice-matched to InAs were grown over a range of 500 to 600°C and 76 or 500 torr using a V/III ratio = 1.1 to 16 and $[AsH_3]/([AsH_3]+[TESb]) = 0.1$ to 0.64 in the gas phase. The best morphology was achieved when grown on a previously grown buffer layer of InAs at a V/III ratio of 7.5 at 500 °C and 200 torr. The growth rate ranged between 0.35 - 2.0 µm/hr for two hour growth times.

Secondary ion mass spectroscopy (SIMS) was used to determine C and O impurity levels and dopant concentrations. The SIMS experiments were performed by Charles Evans and Associates, East, using Cs^+ ion bombardment.

Five crystal x-ray diffraction (FCXRD) using (004) reflection was used to determine alloy composition. Layer thickness was determined using a groove technique and was cross checked by cross sectional SEM. These techniques usually agreed within a few percent.

Room temperature Hall measurements using the Van der Pauw technique were used to determine the majority carrier type and concentration of $AlAs_xSb_{1-x}$ layers grown on semi-insulating GaAs. Contacts were formed by alloying In/Sn (90:10) or In/Zn (95:5) at 300°C to 340°C in a Ar/H_2 atmosphere.

Results And Discussion

The optimum growth conditions for $AlAs_xSb_{1-x}$ occured at 500 °C and 200 torr at a growth rate of 1.0 µm/hour using a V/III ratio of 7.5 assuming a vapor pressure of 0.75 torr for EDMAA at 19.8°C and an [AsH3]/([AsH3]+[TESb]) ratio of 0.13. Lattice matched $AlAs_xSb_{1-x}$ films of high crystalline quality, as evidenced by five crystal x-ray diffraction (FCXRD) (FWHM < 100 arc sec, see Fig. 1a), were obtained. Surface roughness increased for growth rates of 2μm / hr. for the same V/III and [AsH3]/([AsH3]+[TESb]) conditions. The best surface morphologies were obtained by using an InAs buffer layer. GaAsSb cap layers were grown using similar conditions, a V/III of 6, and an [AsH3]/([AsH3]+[TESb]) of 0.07. Hall measurements of $AlAs_{.16}Sb_{.84}$ films 1 μm thick with 200Å $GaAs_{.09}Sb_{.91}$ cap layers grown on GaAs substrates indicated background hole concentrations between 1 to $3x10^{17}$ cm^{-3}. The residual hole concentration of $GaAs_{.09}Sb_{.91}$ films on GaAs ranged between 4 to $7x10^{16}$ cm^{-3}. We were also able to reproducibly obtain lattice matching of AlAsxSb1-x to InAs to within less than 0.015 percent.

The use of non-optimized growth conditions led to several significant problems during the growth of $AlAs_xSb_{1-x}$ layers lattice matched to InAs. These included composition control and reproducibility. Growth at 600 °C resulted in very broad x-ray peaks. The full widths at half of the maximum intensity (FWHM)for the x-ray diffraction peaks were typically ≥ 500 arc seconds. Analysis of the x-ray peak width indicates that it is due to a variation of Sb composition that occurs in the layers as they are grown. The growth of InAs layers at 600 °C after $AlAs_xSb_{1-x}$ layers resulted in Sb incorporation in the InAs. The variation of Sb incorporation into the grown layer is due to the high vapor pressure of Sb deposits on the chamber walls at 600 °C (0.1 torr). Growth at 70 or 500 torr yielded broader x-ray diffraction peaks (FWHM ≥ 300 arc seconds) with less reproducible lattice matching (≤ 500 arc seconds).

We have successfully doped the $AlAs_xSb_{1-x}$ layers both n- and p-type using TESn and DEZn. These results have been discussed in detail previously [4]. We achieved n-type doping levels of 2×10^{17} to $5 \times 10^{18} cm^{-3}$ and p-type levels of 2×10^{16} to $1.4 \times 10^{18} cm^{-3}$.

We used SIMS and Hall measurements of undoped, Zn, or Sn doped $AlAs_xSb_{1-x}$ layers grown on InAs and GaAs to determine the levels of impurities. Both C and O levels in the undoped samples are significantly lower than previously reported results ($\leq 10^{19}$ cm^{-3}). Oxygen levels measured in $AlAs_xSb_{1-x}$ layers are nominally the same regardless of doping or the addition of As. At this point in time it is unclear what the source of the oxygen is in these materials. The oxygen could be coming from contaminants in the source bubblers, background in the reactor or SIMS chamber, or from reaction of the samples with air. The carbon level in undoped and Sn doped $AlAs_{0.16}Sb_{0.84}$ ($\leq 10^{18}$ cm^{-3}) is significantly lower than that found in AlSb (1-2x10^{18} cm^{-3}). This carbon reduction is consistent with the well known effect of increased AsH_3 effectively reducing the incorporation of C in AlGaAs films [12-14]. The higher level of carbon found in the Zn doped $AlAs_{0.16}Sb_{0.84}$ (5x10^{18} cm^{-3}) is most likely related to the DEZn used for doping. It is suspected that the additional carbon is largely responsible for the Hall hole concentration considering the relatively low level of zinc measured by SIMS.

The details of the growth of the InAsSb/InAs multiple quantum well (MQW) structures on InAs have been previously published [15]. The growth conditions used were 500 °C, 200 torr, a V/III ratio of 25 with an [AsH3]/([AsH3]+[TESb]) ratio of 0.75 and a growth rate of 0.9 µm/hour. The composition, x, of the $InAs_{1-x}Sb_x$ quantum wells could be varied between 0.1 and 0.2 by changing the [AsH3]/([AsH3]+[TESb]) flow ratio between 0.81and 0.63 using these growth conditions. The compositions changes can be explained using a thermodynamic model as previously discussed [15].

Although the growth of the $AlAs_xSb_{1-x}$ layers or the quantum well structures by themselves gave uniform and reproducible x-ray diffraction patterns, when the MQW was grown after the growth of $AlAs_xSb_{1-x}$ only a very broad x-ray diffraction pattern was observed. When a layer of InAs was grown after a layer of $AlAs_xSb_{1-x}$, a broad x-ray peak was observed at two theta values greater than the InAs substrates. SIMS measurements indicated the presence of Al in the InAs layer. In order to avoid the incorporation of Al into the quantum well structures, we developed a regrowth technique. Following the growth of the $AlAs_xSb_{1-x}$ layer capped with $GaAs_{1-x}Sb_x$, the quartz reaction chamber was cleaned before growing the MQW structure. A second confinement layer of AlAsxSb1-x could then be grown on top of the quantum wells without affecting the quality of the x-ray diffraction peaks. The highly crystalline quality of the InAsSb quantum wells is confirmed by x-ray diffraction where 7 orders of satellites are observed (Fig. 1(b) and 1(c)) and in optical characterization where the photoluminescence linewidth was 12 meV at 14 K. The background doping of the InAs/InAsSb active region is n-type, $\approx 10^{15}$-10^{16} cm^{-3}.

The band alignments for the MOCVD grown, injection laser are shown in Fig. 2. Following a $GaAs_{0.09}Sb_{0.91}$ buffer, a 2.5 micron thick $AlAs_{0.16}Sb_{0.84}$ cladding is grown on an n-type, InAs substrate. A 200Å, $GaAs_{0.09}Sb_{0.91}$ layer lies between the bottom cladding and a 10 period pseudomorphic MQW consisting of 500 Å InAs barriers and 100 Å $InAs_{0.88}Sb_{0.12}$ wells. A 2.5 μm thick $AlAs_{0.16}Sb_{0.84}$ cladding followed by a 200Å, $GaAs_{0.09}Sb_{0.91}$ contact and oxidation barrier layer is grown on top of the active region. None of the layers were intentionally doped. An (004) x-ray rocking curve for the laser structure is shown in Fig. 1(c). The cladding layer is closely lattice-matched to the substrate ($\Delta a/a = 0.001$), and the entire active region is pseudomorphic with the substrate and cladding layers.

LED and laser emission is observed for a variety of forward bias conditions. No emission is observed in reverse bias. Laser and LED emission spectra (160 K) are shown in Fig. 3. The onset of the LED emission coincides with the energy of the InAsSb quantum well photoluminescence. LED emission has been observed at 300K, 4 μm with ≥ 1 μW peak power (10 kHz, 50% duty-cycle). For LED operation, the cathode $AlAs_xSb_{1-x}$ cladding (A in Fig. 2) is not necessary, but emission intensity is larger in LEDs where the anode $AlAs_xSb_{1-x}$ layer (B in Fig. 2) is thick enough to effectively block electrons from leaving the active region. Gain-guided, stripe lasers were fabricated with Ti/Au metallizations. The facets were uncoated. Devices were tested with 100 nsec pulse widths at 10 kHz (0.1 % duty-cycle). Characteristic of the InAsSb lasers, laser emission was blue-shifted by ≈ 20 meV from the peak of the InAsSb quantum well photoluminescence [1]. The lasers displayed a sharp threshold current characteristic, and lasing was observed through 210 K. Laser emission wavelength was 3.8-3.9 μm. Under pulsed operation, peak power levels ≥ 1 mW/facet could be obtained. A characteristic temperature (T_0) in the 30-40 K range was observed, with the lower value (30 K) being misleading due to degradation of the device.

These maximum operating temperature and characteristic temperature values are comparable to the highest values reported to date, for injection lasers of this wavelength with either strained InAsSb or InAs/GaInSb active regions [1,2,16,17]. Previously, a bipolar laser with a similar, pseudomorphic InAsSb multiple quantum well active region displayed the same characteristic temperature. We believe that the characteristic temperature of both devices is limited by design of the active region and the resulting Auger rates [1]. Further details on emitter characteristics will be presented in subsequent papers.

The use of an internal electron source enables us to consider alternative laser and LED designs that would not be feasible with conventional, bipolar devices. To our knowledge, the only comparable devices are tandem solar cells where tunnel junctions are used to internally generate electrons and holes between stages. Similarly, we can operate several stages of these semi-metal devices in series to produce multi-color LEDs or increase the gain of lasers. As a demonstration, we have grown a 2-stage/ 2-color LED using InAsSb quantum wells with 11% and 13% Sb in each stage. (Each stage is the segment A-B in Fig. 2. A 600Å thick $AlAs_xSb_{1-x}$ electron barrier is between the 2 stages.) Low temperature emission spectra from a 2-stage LED and a 1-stage LED (grown during the same run and removed from growth chamber in the middle of the run) showed two peaks, corresponding to emission from each stage for the 2-stage device. Also, the relative intensities of the peaks of the 2-stage device are comparable to those observed in photoluminescence which indicates that electrons are independently generated in each stage.

In conclusion, we have grown AlSb and $AlAs_xSb_{1-x}$ epitaxial layers by metal-organic chemical vapor deposition (MOCVD) using trimethylamine or ethyldimethylamine alane, triethylantimony and arsine. These layers were successfully doped p- or n-type using diethylzinc or tetraethyltin, respectively. We have demonstrated the growth of high quality $AlAs_xSb_{1-x}$ by MOCVD and used it for optical confinement layers in a 3.8-3.9 μm injection laser with a novel

GaSb/InAs semi-metal electron injector. The laser operated under pulsed conditions up to 210K with a T_o of 30-40K. These operating characteristics are comparable to the best values reported for other injection lasers operating at this wavelength. We have also reported a 2-color LED to demonstrate multi-stage operation of these devices.

Acknowledgments

We wish to thank J. A. Bur and J. H. Burkhart who provided technical assistance. This work was performed at Sandia National Laboratories, supported by the U. S. Department of Energy under contract No. DE-AC04-94AL85000

References

[1] S. R. Kurtz, R. M. Biefeld, A. J. Howard, M. H. Crawford, and M. W. Pelczynski, Appl. Phys. Lett. 68, 1332 (1996).

[2] H. K. Choi and G. W. Turner, Appl. Phys. Lett. 67, 332 (1995).

[3] Y-H. Zhang, Appl. Phys. Lett. 66, 118 (1995).

[4] R. M. Biefeld, A. A. Allerman, and M. W. Pelczynski, Appl. Phys. Lett. 68, 932 (1996).

[5] W. K. Chen, J. Ou, and W-I. Lee, Jpn, J. Appl. Phys. 33, L402 (1994).

[6] D. S. Cao, Z. M. Fang, and G. B. Stringfellow, J. Crystal Growth, 113, 441 (1991).

[7] G. J. Bougnot, A. F. Foucaran, M. Marjan, D. Etienne, J. Bougnot, F. M. H. Delannoy, and F. M. Roumanille, J. Crystal Growth, 77, 400 (1987).

[8] M. Leroux, A. Tromson-Carli, P. Gibart, C. Verie, C. Bernard, and M. C. Schouler, , J. Crystal Growth, 48, 367 (1980).

[9] C. A. Wang, M. C. Finn, S. Salim, K. F. Jensen, and A. C. Jones, Appl. Phys. Lett. 67, 1384 (1995).

[10] C. A. Wang, K. F. Jensen, A. C. Jones, and H. K. Choi, Appl. Phys. Lett. 68, 400 (1996).

[11] E. T. R. Chidley, S. K. Haywood, R. E. Mallard, N. J. Mason, R. J. Nicholas, P. J. Walker, and R. J. Warburton, J. Crystal Growth, **93**, 70 (1988).

[12] G. B. Stringfellow, "Organometallic Vapor Phase Epitaxy:Theory and Practice" (Academic Press, Inc., San Diego, CA, 1989).

[13] M. A. Tischler, R. M. Potemski, T. F. Kuech, F. Cardone, M. S. Goorsky, and G. Scilla, J. Crystal Growth, **107**, 268 (1991).

[14] W. S. Hobson, T. D. Harris, C. R. Abernathy, and S. J. Pearton, Appl. Phys. Lett., **58**, 77 (1991).

[15] R. M. Biefeld, K. C. Baucom, and S. R. Kurtz, J. Crystal Growth, **137**, 231 (1994).

[16] A. A. Allerman, R. M. Biefeld, and S. R. Kurtz, Appl. Phys. Lett., **to be published July** (1996).

[17] . R. H. Miles (private communication).

Figure Captions

Figure 1. X-Ray diffraction spectra of (a) 2.5 μm of AlAsxSb1-x lattice matched to InAs, (b) a 10 period pseudomorphic $InAs_{0.88}Sb_{0.12}$/InAs quantum well active region, and (c) an injection laser using the same active region as (b) and 5 μm of $AlAs_{0.16}Sb_{0.84}$ cladding.

Figure 2. Schematic of the structure and heterojunction band alignments for the MOCVD-grown, semi-metal electron injection laser. Multiple stages are possible by repeating the injector/active region cell illustrated between A and B. Forward bias polarity is indicated in the figure.

Figure 3. Laser and LED emission spectra at 160 K.

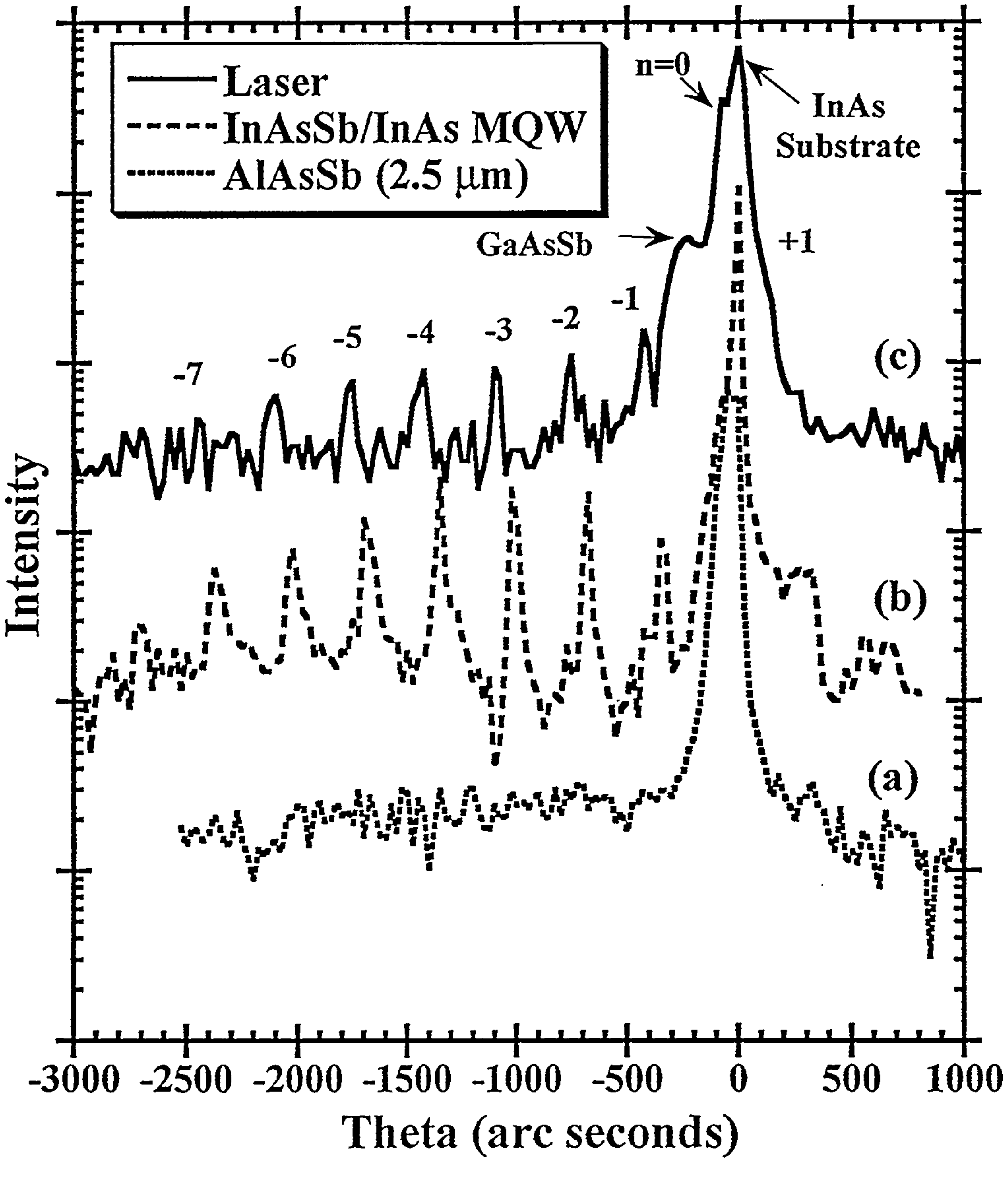

Laser
InAsSb/InAs MQW
AlAsSb (2.5 μm)
n=0
InAs
Substrate
GaAsSb
+1
-1
-2
-3
-4
-5
-6
-7
(c)
(b)
(a)
Intensity
-3000
-2500
-2000
-1500
-1000
-500
0
500
1000
Theta (arc seconds)

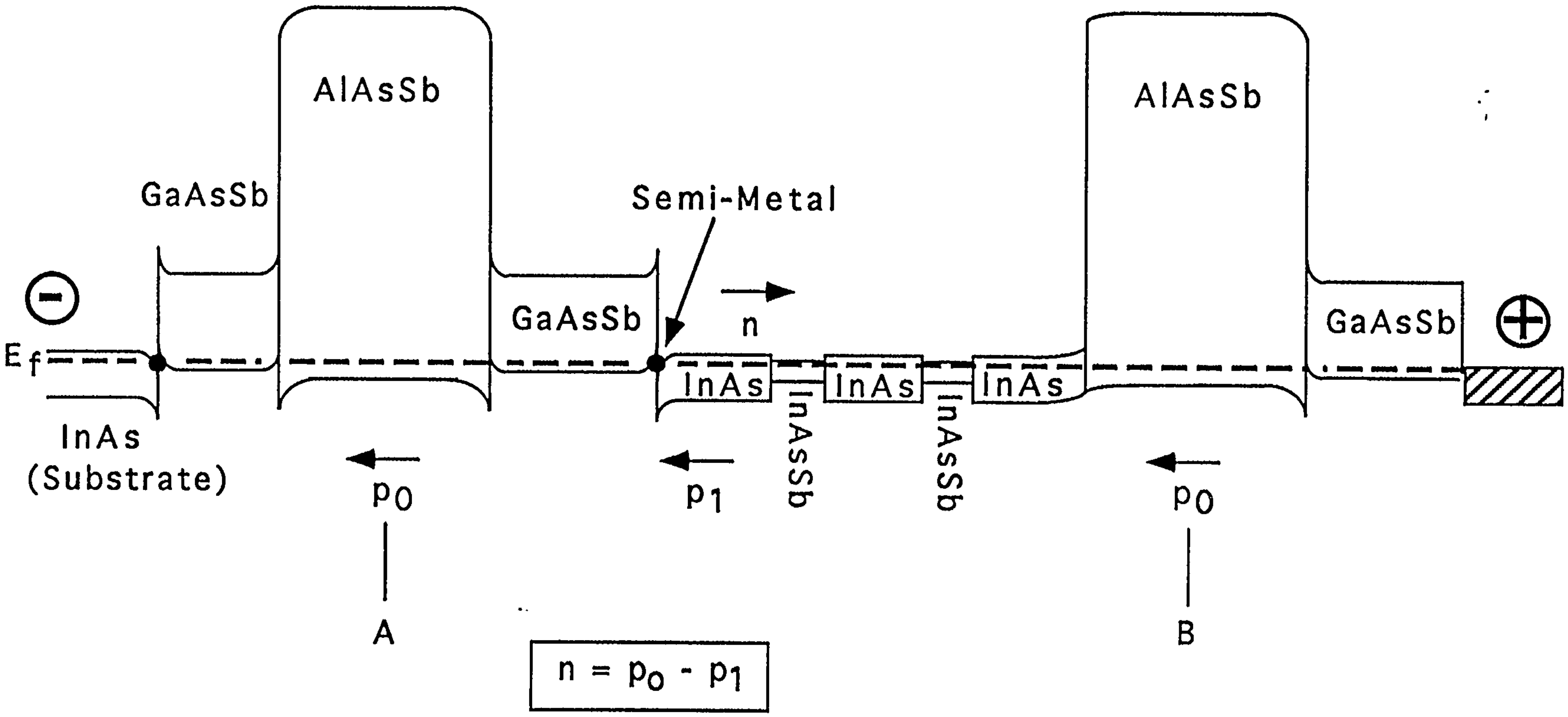
AlAsSb
AlAsSb
GaAsSb
Semi-Metal
GaAsSb
n
GaAsSb
E_f
InAs
InAs
InAs
InAs
(Substrate)
InAsSb
InAsSb
p_0
p_1
p_0
A
B
$n = p_0 - p_1$

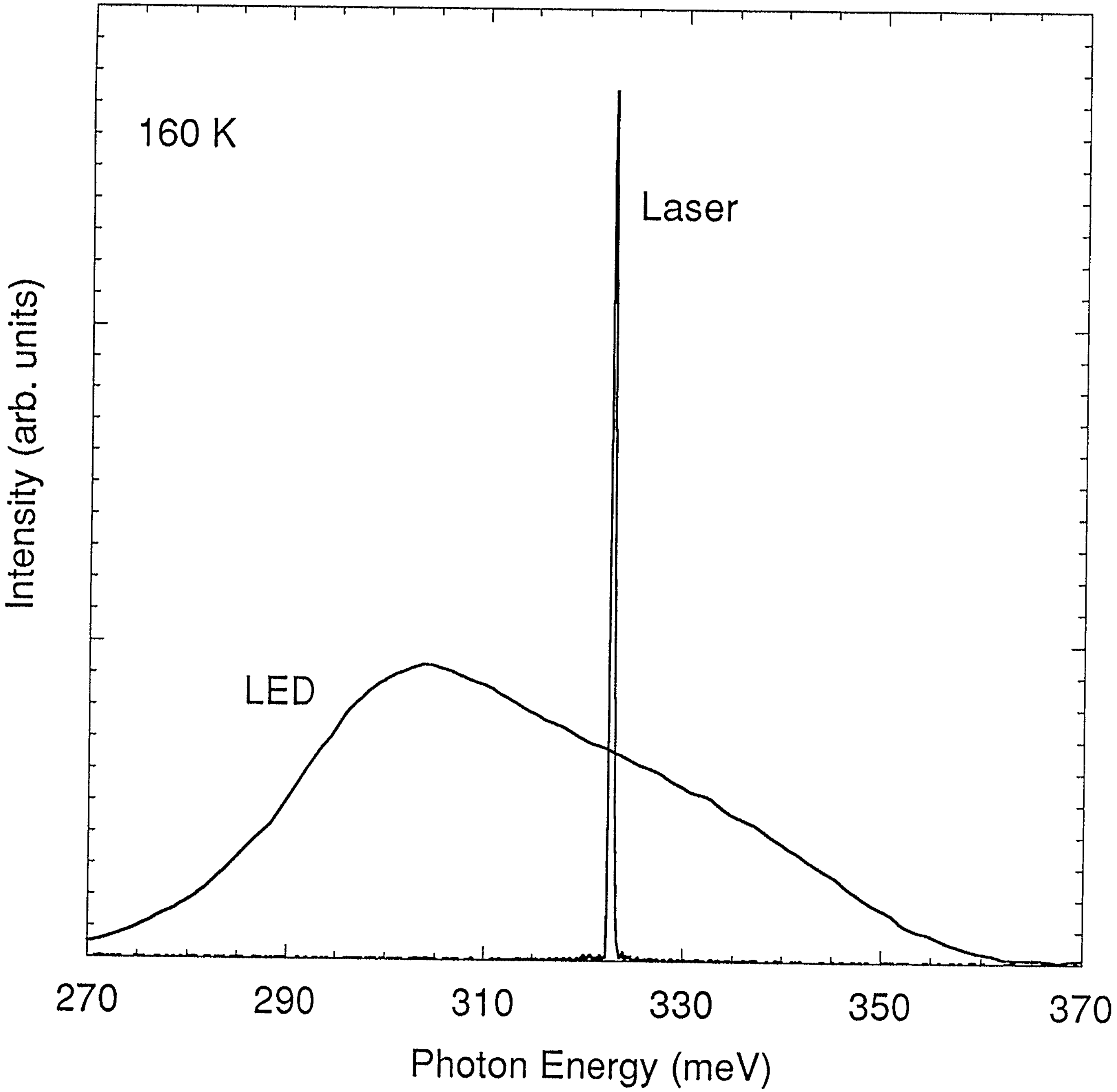
160 K
Laser
LED
Intensity (arb. units)
270
290
310
330
350
370
Photon Energy (meV)